UDC 551.511.6:551.551.2:551.584.2

Mesoscale Wind Fields and Transport Estimates Determined From a Network of Wind Towers[1]

LARRY L. WENDELL—*Air Resources Laboratories, Environmental Research Laboratories, NOAA, Idaho Falls, Idaho*

ABSTRACT—Techniques are developed to utilize wind data from a network of stations to study mesoscale flow patterns and transport in the lower planetary boundary layer. The data sample for this study is hourly averaged wind data for the year 1969 from 21 stations over the Upper Snake River Plain of southeastern Idaho. Examination of 6-hourly wind field plots for the entire year reveals a strong correlation of the flow patterns with a topographic variation of relatively minor amplitude. Plots of patterns of trajectories of hypothetical "particles" released once an hour from a single location for the entire year are typed according to season and release period during the day. These patterns provide an estimate of a transport climatology; a climatology not available from a wind rose at the source. Evidence is presented that demonstrates that estimates of transport from the source wind can be seriously in error due to marked spatial variations in the flow.

1. INTRODUCTION

A great deal of theoretical, numerical, and observational work has been done on the vertical wind structure of the planetary boundary layer. An historical outline, with references to the modeling developments, has been presented (Ching and Businger 1968). These models all include the assumption of horizontal uniformity in the flow. In some recent work, Bonner and Paegle (1970) developed a model in which the eddy viscosity and pressure gradient force are both allowed to vary over sloping terrain. This work also includes 1 week's observations of horizontal variation of the wind and pressure. Much of the recent modeling has been done in an attempt to explain observational evidence of a low-level jet in the wind profile in the planetary boundary layer (Blackadar 1957, Hoecker 1963, 1965). Another phenomenon of the flow in the planetary boundary layer that has been deduced by direct observation (Angell et al. 1968) and by indirect observation (Hanna 1969) is the system of helical roll vortexes that seems to occur in strong straight flow over flat terrain under thermally unstable conditions. A model for this phenomenon has recently been developed and tested (Brown 1970).

Indeed, the recent expansion of knowledge of the vertical structure of wind flow in the planetary boundary layer has been impressive. It may have provided some of the incentive for work done by diffusion meterologists on the effects of vertical variation of the wind on atmospheric diffusion (Saffman 1962, Pasquill 1962, Smith 1965, Gee 1967). It has been pointed out, however, that horizontal variation of the wind in the boundary layer on a microscale or mesoscale has not received nearly as much study (Slade 1968). In microscale atmospheric diffusion experiments (within a few kilometers), transporting velocities are estimated by averaging the source wind over the period of the experiment. In one noted mesoscale (10–100 km) diffusion experiment (Pasquill 1962), the transporting velocities showed little downstream variation. At the present time, the most common operational practice for estimating the diffusion of a pollutant from a single source involves only the wind at the source. Graphs exist that allow estimates of downwind concentrations up to 100 km distant (Hilsmeier and Gifford 1962), but this should not necessarily be taken to infer that the travel is over a straight path.

The problem, simply stated, is to what extent the wind, observed at a single location, may be used to represent the wind over an area. For transport considerations, the observation should be a time average over a short interval to remove local turbulent fluctuations. Obviously, the answer to this question will depend upon the size of the area. For the large scale (more than a few hundred kilometers), there is often a very striking spatial variation in the horizontal flow. This is not usually the case for small-scale flow except under extremely light wind conditions.

In an attempt to determine the nature of the mesoscale horizontal variation of the wind in the lower portion of the planetary boundary layer, we recorded wind data from a randomly spaced collection of 21 stations within an area of 12,420 km^2 (4,800 mi^2) beginning on Jan. 1, 1969. There are many objective and statistical computational schemes that may be applied to a data sample of this type. However, as a preliminary approach, a technique for producing inexpensive computer plots of the wind data along with wind vectors objectively interpolated to a regular grid provides a convenient display of the data for visual examination of space and time variation in the flow patterns (Wendell 1970, Mancuso and Endlich 1970). A display of this type with the major topographic features superimposed also allows visual correlation of the flow patterns with underlying terrain. To estimate transport from the wind field data, we developed a technique for

[1] The work described in this paper is supported by an agreement with the Division of Reactor Development and Technology, U.S. Atomic Energy Commission.

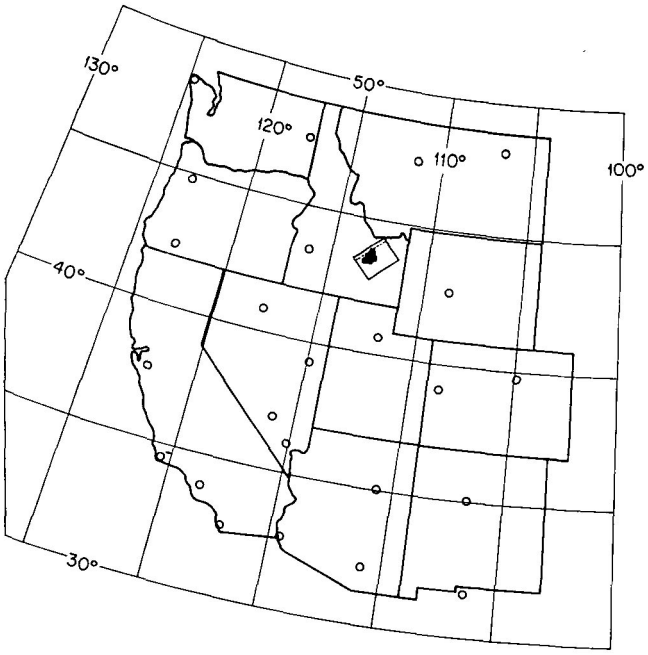

FIGURE 1.—Location and extent of computational grid for mesoscale wind observations. The solid border of the rectangular box in southeastern Idaho contains all the observation locations, but no calculations are carried out for the area northwest of the dashed line. The solid black area represents the geographical extent of the National Reactor Testing Station.

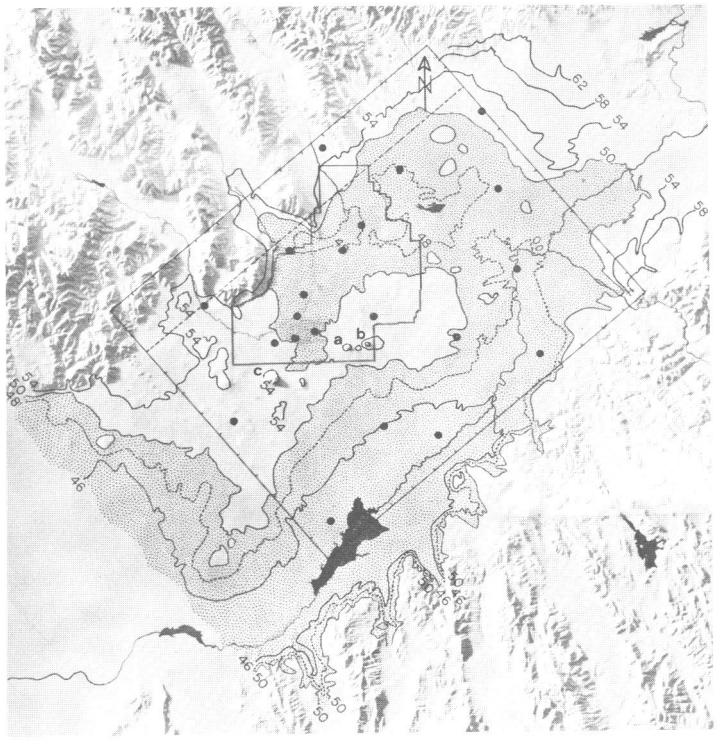

FIGURE 2.—Relief map of the Upper Snake River Plain in southeastern Idaho. The values shown on the few contour lines over the plain are in hundreds of feet. The stippled area within and adjacent to the grid indicates the area of altitude less than 5,000 ft MSL. The tick marks along the border of the grid indicate the grid-point separation, 5.33 mi. The letters a, b, and c show the location of three prominent buttes. The solid dots indicate the location of the wind towers.

computing and displaying, in a compact form, trajectories of hypothetical particles released, one per hour, from a single source. The trajectory plots may also serve as a tool for quickly discerning space and time changes in the flow pattern.

Both wind field and trajectory plots have been produced for the entire year of 1969 (Wendell 1970). This information provides the basis for subjective classification of trajectory pattern types and a determination of their frequency of occurrence on a seasonal basis. The implications of these types on transport are considered.

2. DESCRIPTION OF THE AREA

The National Reactor Testing Station (NRTS) of the Atomic Energy Commission (AEC) is located along the western edge of the Upper Snake River Plain in southeastern Idaho. The scale of concern in this work is shown by an outline of the computational grid (rectangular box in southeastern Idaho) on a map of the western United States in figure 1. The NRTS is represented by the black area within the computational grid. The size of the grid shown is 85.7 km wide and 129.6 km long. The circles on the map indicate the locations of the routine upper air sounding stations. This figure shows that the scale of concern in this work is about an order of magnitude smaller than the generally accepted synoptic scale.

The topography of the area is shown in figure 2. The severe height variation of the mountainous terrain is shown only qualitatively through a shadowed photograph of a relief map. The gentle height variation over the relatively flat plain area is depicted by the height contours. The area in which the terrain height is less than 5,000 ft is stippled to emphasize the major features of the comparatively mild terrain height variation. The relatively flat expanse of the plain is broken by three buttes. Two of them, identified by the letters "a" and "b" in figure 2, are each about 1 mi in diameter at the base and about 1,500 ft higher than the surrounding terrain. The third butte, identified by the letter "c" in figure 2, is about 3 mi in diameter at the base and about 2,700 ft higher than the surrounding terrain. The solid line which forms the rectangular box encloses the area in which data is collected. The solid black dots show the locations of the wind towers. The dashed line indicates the northwest boundary of the area of wind field and trajectory calculations. This was established because of the rugged nature of the terrain to the northwest. The mountains to the northwest and southeast, which form the boundaries of the upper plain, prompted the 49° rotation of the computational grid. The irregular border within the boundary encloses the NRTS.

Probably the most striking feature of the mild variations in topography is the interruption of the southwestward slope of the plain by the higher ground (above 5,000 ft) jutting out from the mountains to the northwest. It has the effect of creating a fishhook-shaped depression that proceeds northeastward along the Snake River up the right-hand side of the grid, then northwestward across the top of the grid, and finally southwestward along the left-

hand side of the grid ending in the southern portion of the test site. Other features of note are the three valleys, almost perpendicular to the northwestern boundary of the test site, and the marked change in terrain gradient from left to right at the top of the grid. The greatest height variations over the computational grid, excluding the three buttes and the mountains on the boundaries, indicate slopes of about 0.075. The mountain slopes average about 0.25–0.30.

3. DATA COLLECTION AND REDUCTION

The station locations within the boundaries of the NRTS were established years ago by the needs of the AEC. The others were placed more in accordance with the needs of the present study and economic feasibility. Each station consists of a 15.2- to 76-m tower, wind direction and speed measuring equipment, and a recorder. Three of the stations also have temperature sensing equipment. Information pertaining to the type of data measured and the height of the measurements at each station is available (Wendell 1970). The wind speed and direction data used in this work were averaged to eliminate higher frequency fluctuations that would contribute more to dispersion of material than to its transport. Since the data were manually reduced from strip charts, a compromise with economy required an averaging interval no shorter than 1 hr. An extensive error analysis was performed on the reduced data (Wendell 1970).

4. RANDOM- TO GRID-DATA ANALYSIS

For convenience in numerical computations involving the data from these randomly spaced wind stations, an objective interpolation scheme was applied to obtain wind components on a regularly spaced grid. The technique involved uses a weighted average of the velocity components from several of the stations nearest each of the gridpoints. This approach has been discussed previously (Shepherd 1968, Van der Hoven 1968, 1969). For the data presented here, the interpolation scheme may be represented as

$$\bar{u}_{i,j}=\frac{\sum_{k=1}^{N}\frac{u_k}{r_k^2}}{\sum_{k=1}^{N}\frac{1}{r_k^2}}$$

and (1)

$$\bar{v}_{i,j}=\frac{\sum_{k=1}^{N}\frac{v_k}{r_k^2}}{\sum_{k=1}^{N}\frac{1}{r_k^2}}$$

where $\bar{u}_{i,j}$ and $\bar{v}_{i,j}$ are the cross-valley (x) and up-valley (y) components of the wind obtained at point (i, j) on the grid, u_k and v_k are the x- and y-components at a wind station a distance of r_k away from the gridpoint (i, j), and N is the number of stations in the average.

In all the analyses shown in this work, the minimum number of stations used in the average at any gridpoint was required to be three, regardless of their distance away. If there were more than three stations within a radius of 17.16 km (two grid units), they were also used in the average. Since the station locations are fixed and usually many hours of data are available for analysis, a table for each gridpoint of the 10 closest stations and their distances from the gridpoint in ascending order is established and stored before the interpolation process begins. Then, as the wind is available for analysis, the list of stations for each gridpoint is scanned, and the first three stations with available data are selected. If the next station in the list has data available and is less than the specified distance of 17.16 km from the gridpoint, it is also used in the average. Each station in the list is checked like this until one is encountered that lies outside the limiting distance. This method is applied at every gridpoint, including the boundaries. Thus, for some gridpoints, the method is an interpolation, and for others, it is an extrapolation.

There are random- to grid-wind interpolation schemes that involve, as a weighting factor, the angle which the wind direction at the station makes with the line connecting the station and the gridpoint (Endlich and Mancuso 1968). This approach, however, which weights upstream and downstream stations more heavily than cross-stream stations, is based on the jet stream characteristics of large-scale flow that does not necessarily apply to mesoscale flow. Also, no physical constraints such as continuity were imposed on the wind field. No unreasonable vertical velocity estimates have resulted from divergence calculations using the interpolated wind data.

The wind components, when obtained at the gridpoints, are now ready for use in various types of analyses. However, they may also be used to enhance the appearance of a plot of the raw data for visual observation. A plot program has been developed in which the hourly averaged data may be displayed at any time interval in a fashion that allows the wind fields to be scanned like a series of synoptic weather maps. Wind fields at 6-hr intervals for the entire year of 1969 have been plotted for examination (Wendell 1970). The definitions of the symbols used in the plots are shown in table 1.

5. SOME TYPICAL TYPES OF FLOW PATTERNS

The 6-hourly plots were arranged in such a way that they could be scanned visually. One can deduce much more about the types of flow patterns that occur from a long series of wind field plots than from a set of wind roses at each of the stations.

The most interesting feature observed is the strong correlation of the wind patterns to the large fishhook-shaped depression in the topography over the grid. When the contour level outlining this depression is superimposed on the wind fields, varying degrees of this conformity can be observed during about 57 percent of the days of the year. This relationship varies from a high of 63 percent during the spring to a low of 42 percent during the fall. Selected examples of this phenomenon are shown in figure

TABLE 1.—*Definitions of symbols used in wind field plots*

Symbols at wind stations		Symbols at gridpoints	
Symbol	Definition	Symbol	Definition
Standard shaft and barb	Wind direction and speed. (Each barb represents 10 mi/hr.)	→	Wind speed and direction. (Distance between gridpoints represents 25 mi/hr.)
*	A direction change of 90° or greater during the averaging hour	→	$2<\|V\|<5$ mi/hr
+	Missing data	–	$\|V\|<2$ mi/hr
0	Calm	0	Calm

3 for each of the four seasons. In the absence of other dynamic effects, this type of flow might be expected to occur simply through the channeling of a light southwesterly flow entering the lower end of the plain. Another qualitative explanation of this phenomenon, at least during the warmer seasons, might be as follows: during synoptic conditions in which the pressure gradient over the area is weak and the major driving force for the air motion is gravity, daytime heating would cause the flow over the plain to be from the lower terrain southwest of the computational grid to the higher terrain northeast of the computational grid. As the cooling process begins in the evening, the tendency to reverse the direction of the flow along the top of the grid is much stronger on the northwestern half because of the steeper terrain in that area. Thus, the inertia of the southwesterly flow is overcome sooner there, and the flow becomes northeasterly into the portion of the depression that extends southwestward over the test site. This is probably not the only cause of the phenomenon, but one would expect it to be a major one.

A further refinement of the phenomenon just described was observed during about 12 percent of the days during 1969. This is the situation in which the conditions are suitable for the formation of a circular-shaped eddy that would persist for a few hours in the upper portion of the grid. A few examples of this eddy, one for each season, are shown in figure 4. This condition occurs primarily at night and most frequently during the summer. This would indicate that it is most closely, but not entirely, associated with the diurnal heating cycle and local topographic features.

The flow patterns just described are interesting because they are examples of organized spatial variations in the flow pattern. They would be extremely difficult, if not impossible, to determine from wind rose plots at several locations. This type of spatial variation in the flow is very important because of its implications in the transport of material over the area.

The type of flow that can be represented easily by the winds at a single location does occur over the Upper Snake River Plain in the form of episodes of strong south-through-southwesterly flow or strong north-through-northeasterly flow. The uniform flow with the strong (average greater than 10 m/s) southerly component was observed during some portion of about 14 percent of the days in 1969. The uniform flow with the strong northerly component was observed about 7 percent of the days in 1969. Occasionally, the S–SW winds were prefrontal and the N–NE winds were postfrontal, but in the majority of the cases they were both associated simply with strong pressure gradients. Examples of both of these types of flow are shown in figures 5 and 6.

Another characteristic of the flow that has been observed, but less frequently than any described previously, is channeled flow from one or more of the three valleys northwest of the grid. Two examples of this are shown in figure 7. The sequence during the early morning hours of March is an example of a strong wind situation, and the sequence during the late evening in November is an example of a light wind situation. A wind rose for the station in the valley northwest of the grid shows down-valley flow in excess of 7 m/s about 5 percent of the time. This is an indication of the relatively infrequent occurrence of episodes showing a sustained effect, by this phenomenon, on the flow pattern over the plain.

Probably the most dramatic occurrence observed in the flow pattern is the passage of a definitive frontal system. In this case, as in the case of the sustained strong uniform winds over the grid, the effect of the relatively mild terrain variation over the grid is hardly discernible. One example of such a passage is shown in figure 8. The winds observed at 1300 MST on May 30, 1969, are from the southwest generally in excess of 13 m/s over most of the grid. The station in the valley just north of the site boundaries gives the first indication of the approaching front, which then moves across the grid from the northwest in a matter of about 9 hr. There are weaker indications of frontal passages during the year, however. Those having the intensity of the example here occur during about 3 percent of the days of the year with a high of around 7 percent in the spring.

The features in the flow patterns presented here serve to illustrate that the expanded point of view provided by a display of a network of wind observations can be a valuable tool in studying mesoscale as well as large-scale phenomena. Information gained from this type of data presentation should be useful in improving local wind forecasts.

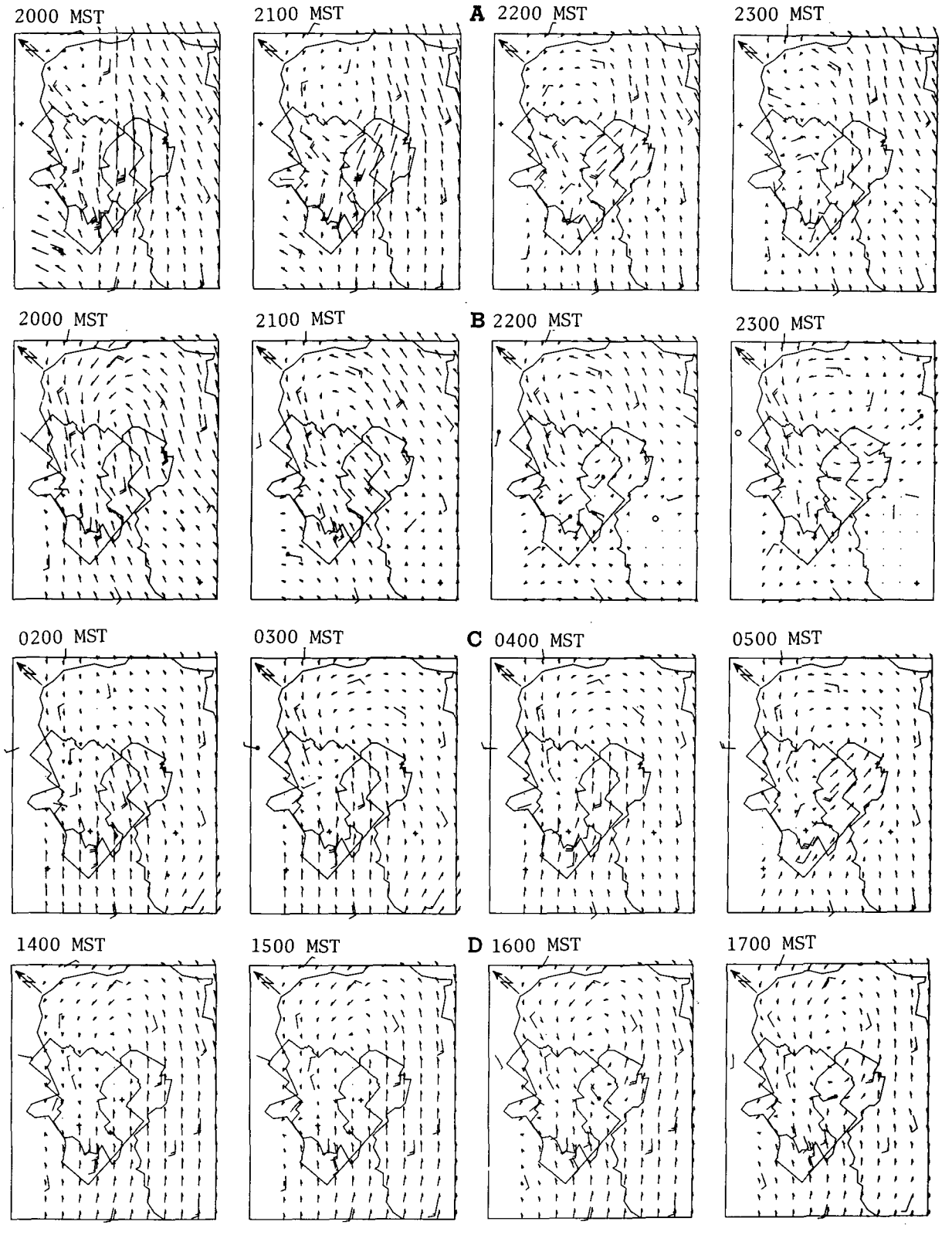

FIGURE 3.—Examples of the flow pattern over the grid conforming to the topography. A 4-hr series is shown for each season of the year, (A) winter (Feb. 9, 1969), (B) spring (May 13, 1969), (C) summer (Aug. 6, 1969), and (D) autumn (Nov. 18, 1969). The 5,000-ft contour is included for reference purposes (fig. 1). The wind data from each station are plotted in standard form and the interpolated winds are plotted as vectors at each gridpoint (table 1).

6. TRANSPORT

Another use of the wind components at the gridpoints is to provide an indication of the transport by the wind over the grid. The variation of the wind field over the grid, which is observed in the wind field plots, seems to provide convincing evidence that advection of material for more than a few hours or a distance of 15–30 km with the wind

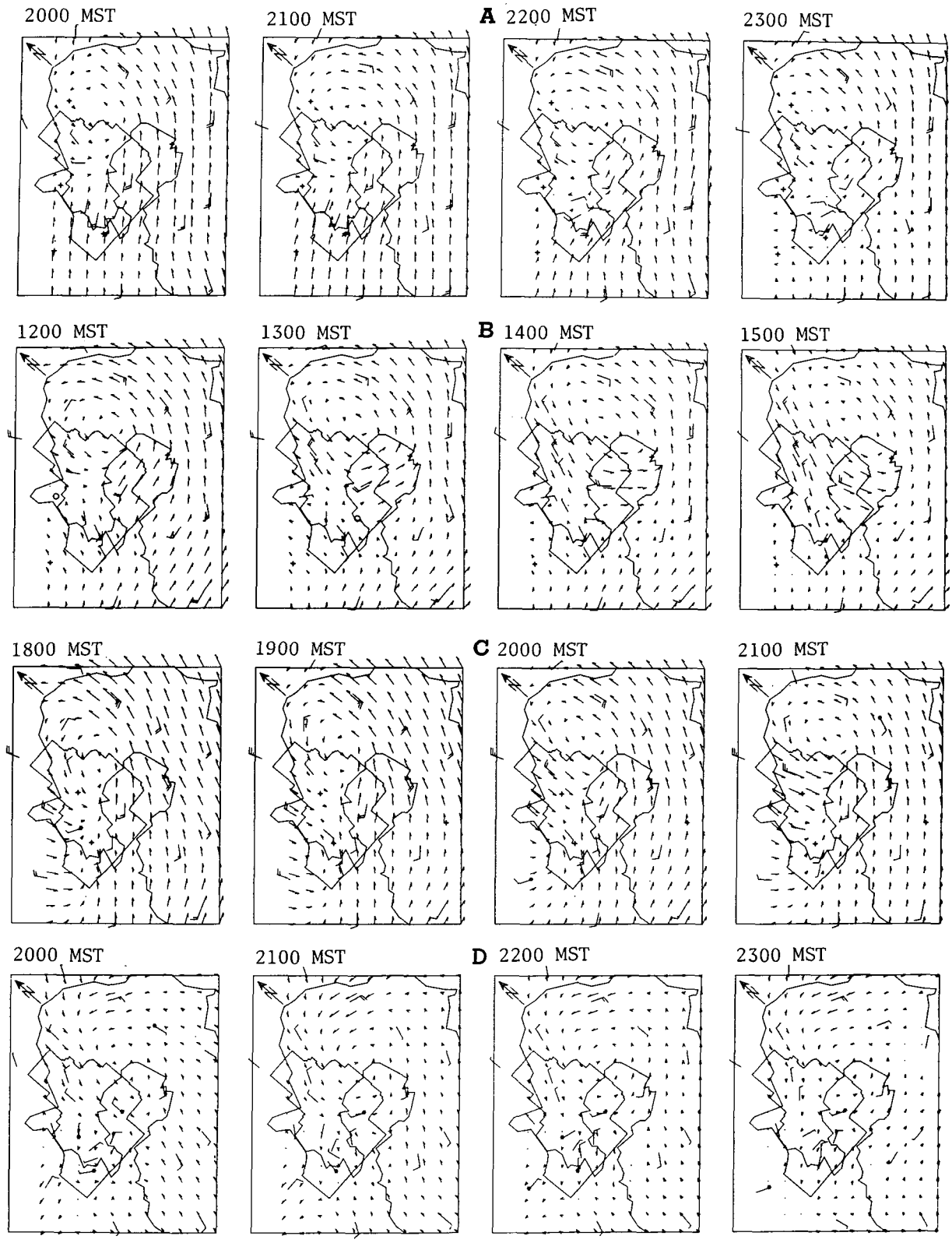

FIGURE 4.—Examples of a cyclonic eddy in the upper portion of the grid. A 4-hr series is shown for each season, (A) winter (Jan. 8, 1969), (B) spring (Mar. 6, 1969), (C) summer (June 24, 1969), and (D) autumn (Nov. 18, 1969). See figure 3 for other details.

measured at the source can be misleading. The improved horizontal resolution in the data by measurements spaced over the grid should obviously produce a better representation of atmospheric transport. It should be kept in mind, however, that the transport represented by the wind measurements from these towers is restricted to an atmospheric layer in which these measurements are representative.

The height of this layer will depend entirely on vertical variation in the direction and speed of the wind. The nature of the vertical variation or shear in the wind speed

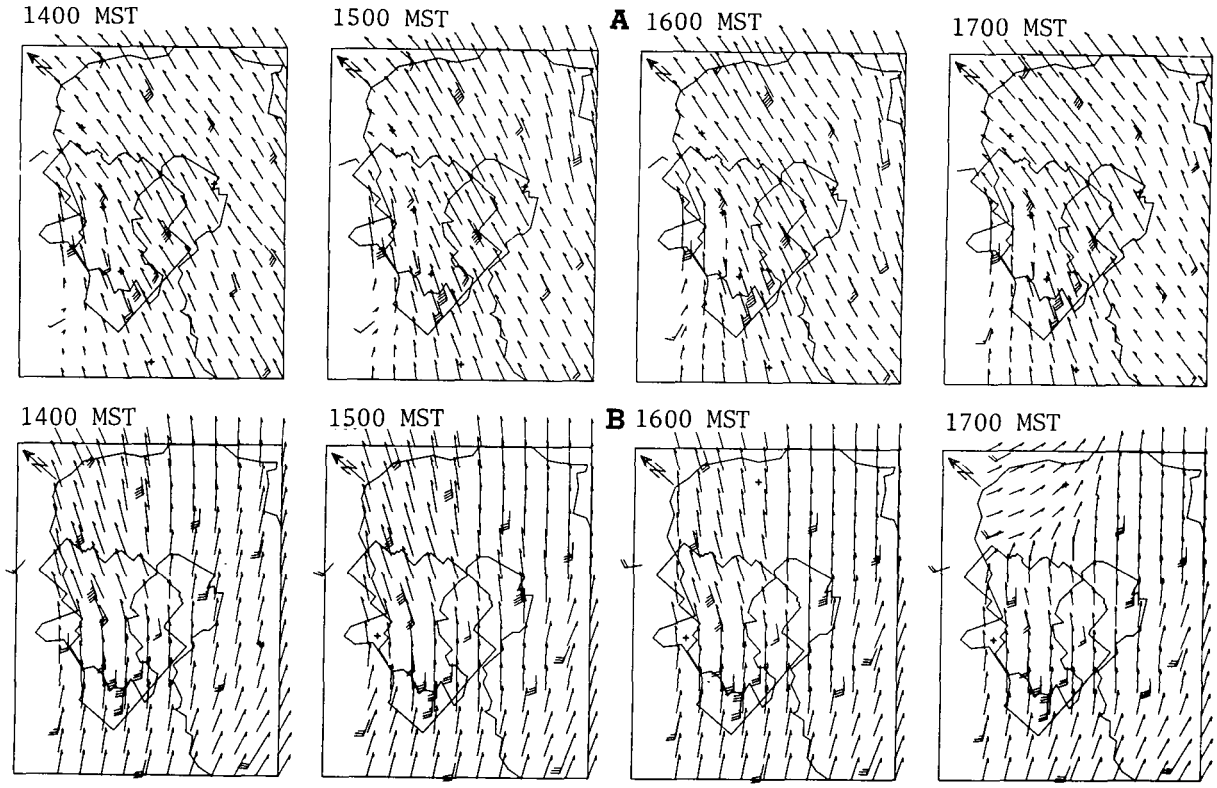

FIGURE 5.—Examples of a strong, sustained, uniform flow with a large southerly component. A 4-hr series is shown for (A) Jan. 19, and (B) July 3, 1969. See figure 3 for other details.

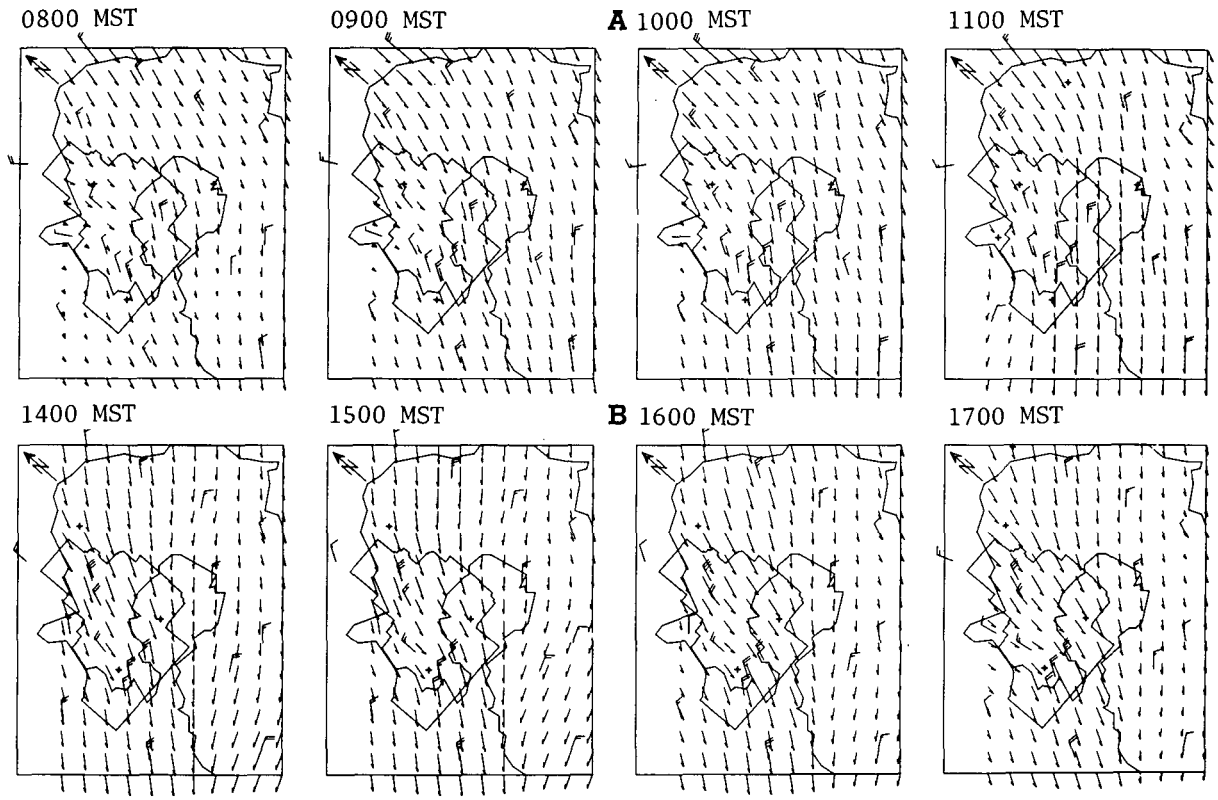

FIGURE 6.—Examples of a strong, sustained, uniform flow with a large northerly component. A 4-hr series is shown for (A) May 7, and (B) Oct. 18, 1969. See figure 3 for other details.

and direction will depend on the roughness of the surface, the atmospheric temperature profile, and, to some extent, the large-scale motion and weather patterns moving through the area. The wind variation with height at the NRTS has been observed under several conditions and is found to range from the classical logarithmic profile to a

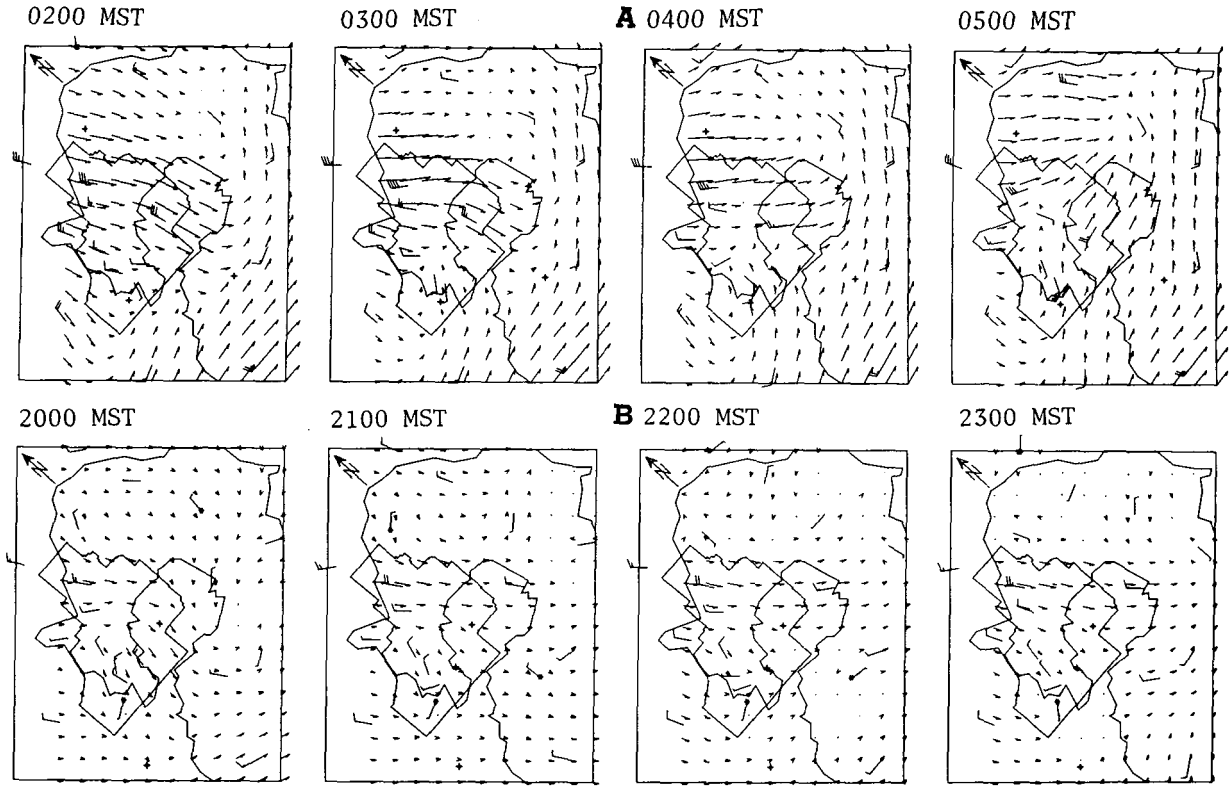

FIGURE 7.—Examples of a valley wind extending significantly over the plain. A 4-hr series is shown for (A) Mar. 19, and (B) Nov. 17, 1969. See figure 3 for other details.

profile that showed a 150° direction shear between 6 and 9 m above the ground. This strong shear has been observed several times during the early morning hours on a tower located in the tip of the fishhook-shaped depression shown in figure 2. It is attributed to the fact that the slope of the terrain in this area is opposite the general slope of the terrain over the upper Snake River Plain. The general downslope drainage is, therefore, opposed by this local anomaly in the topography. Since this strong shear has never been observed to extend above about 9 m and the wind observation heights were above 15 m, it should have no effect on the transport calculations for a layer between 9 and 150 m.

To depict transport by the winds over the grid, we constructed the trajectories of a series of "particles," released sequentially from a selected spot on the grid, using the recorded hourly averaged data interpolated to the regular grid. The technique for constructing the trajectories involves an interpolation of the velocity components from the gridpoints to the particle positions and a purely advective scheme for moving the particles. A linear interpolation in time is used between hourly averaged wind fields. The time interval used between each advection step is 10 min. (A 5-min advection step produced no significant difference in a test set of trajectories. A reduction of the grid spacing also produced no significant difference in the trajectories.)

The scheme for graphical representation of the trajectories is depicted in figure 9. These two series of trajectories indicate the paths of 12 particles released 1 hr apart from a location in the southern part of the NRTS. The initial release times are shown at the top of the plots. The numbers at the ends of the trajectories indicate the order in which they are released. The letters along the trajectories indicate the locations of the particles at hourly intervals after release. The letter "A" occurs 1 hr after the initial release, the letter "B," 2 hr, and so on. Like letters may be connected to form a streak line and may be used to approximate a plume center line. The appropriate columns of table 2 may be used to determine position times for the releases shown in figure 9. Note that two plots are used to show the transport for each 24-hr period. The first plot depicts the trajectories for a series of releases from 0100 through 1200 MST with advection continuing to 2400 MST, if there are any particles left within the grid boundaries. The second plot depicts the trajectories for a series of releases from 1300 through 2400 MST the same day with advection continuing, if particles are still on the grid, to 1200 MST the next day. The overlap allows one to estimate the continued transport of the last few particles, which might be left on the grid, from the first trajectory of the next plot. Thus, one may observe the transport continuously for as long a period of time as his data sample provides.

The display format shown in figure 9 has been used to show the trajectories for a continuous hourly release of particles from a location in the southern portion of the test site for the period from 0100 MST on Jan. 1, 1969, through 2400 MST on Dec. 30, 1969 (Wendell 1970). The dots on the diagrams represent a few population centers in the area and may be used as reference points. Examination of the series of trajectory plots for 1969 reveals a substantial variety of trajectory patterns. In several cases, however, the patterns are similar enough to be recognized as rela-

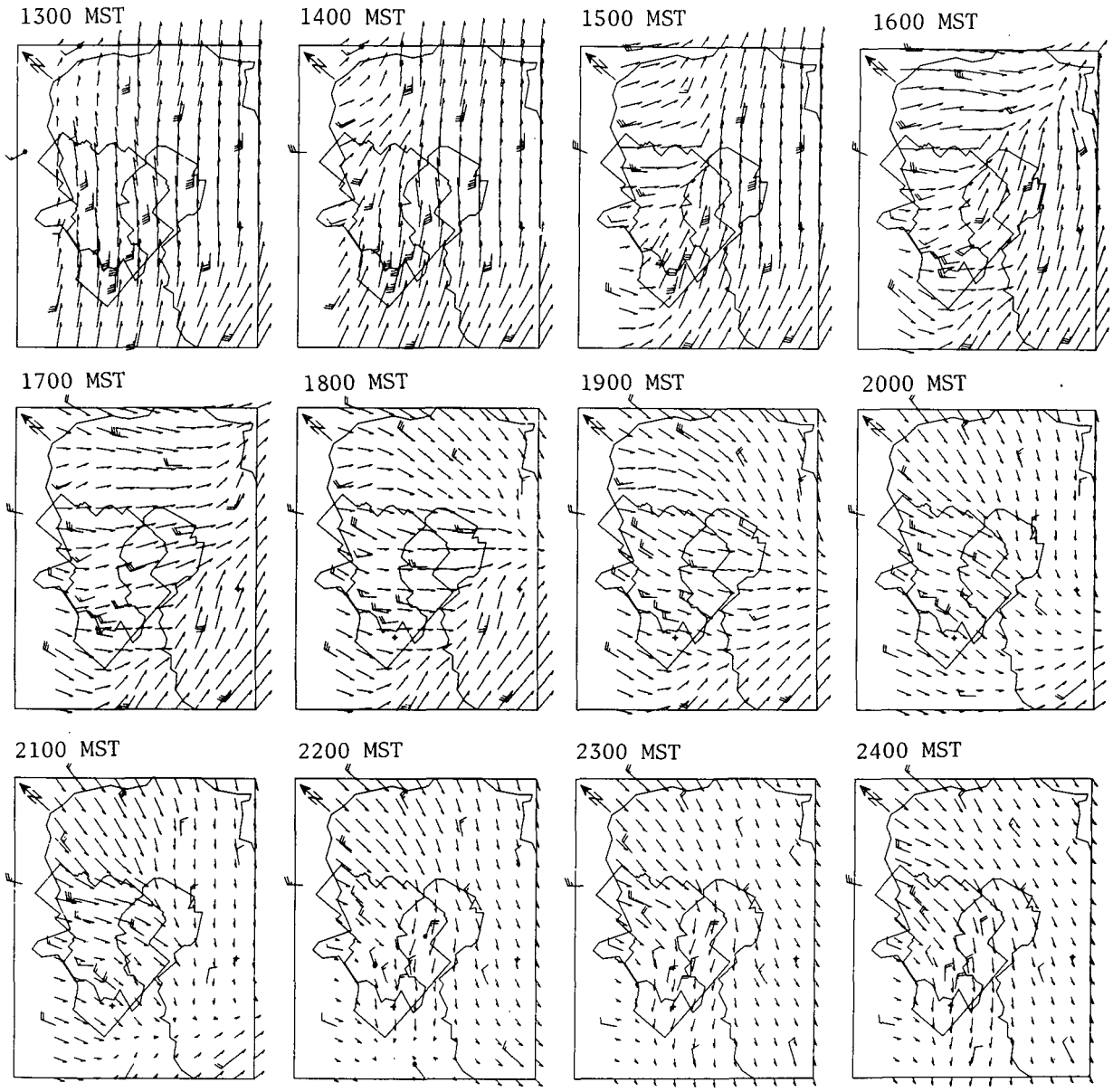

FIGURE 8.—Example (May 30, 1969) of the effect of a frontal passage on the flow pattern over the grid. See figure 3 for other details.

tively distinct types. A few of the more common types are shown in figure 10. The percentages of occurrence of these types were determined by subjective visual examination and are shown in table 3.

The most common pattern of trajectories for the entire year, regardless of release times, is designated as type "A" and is characterized by a southwesterly movement of all 12 particles released, with little deviation until they leave the bottom boundary of the computational grid. This is an indication of a sustained northeasterly flow from the source to the boundary for the duration of the release period. Considering the entire year, we find that the variation in the percentages of occurrence is small enough to indicate very little preference for one release period or the other. This also seems to be true for each individual season except winter, in which the 0100–1200 MST release period holds a significant edge. This type of transport pattern has its maximum occurrence in the winter and its minimum occurrence in summer. In fact, this pattern is the predominant type of each season except summer, during which time it ranks fourth and fifth for the 0100 and 1300 MST releases, respectively. During the winter season of 1969, this pattern persists for periods up to 8.5 days.

The next most persistent type on an annual basis is denoted type "B" and is recognized by the steady procession of particles in a northerly direction directly off the left boundary of the grid. This would be caused by a sustained southerly flow lasting throughout the entire release period. This type, like type A, shows no particular preference for either release period. This type shows a maximum occurrence of 16 percent during the winter, and it ranks as the second most frequent type during this season. The only other significant occurrence of this type is in the fall (8 percent), and it ranks fourth and second for the 0100 and 1300 MST releases, respectively.

The third pattern, designated type "C," is the first to indicate a change in the flow during the release period.

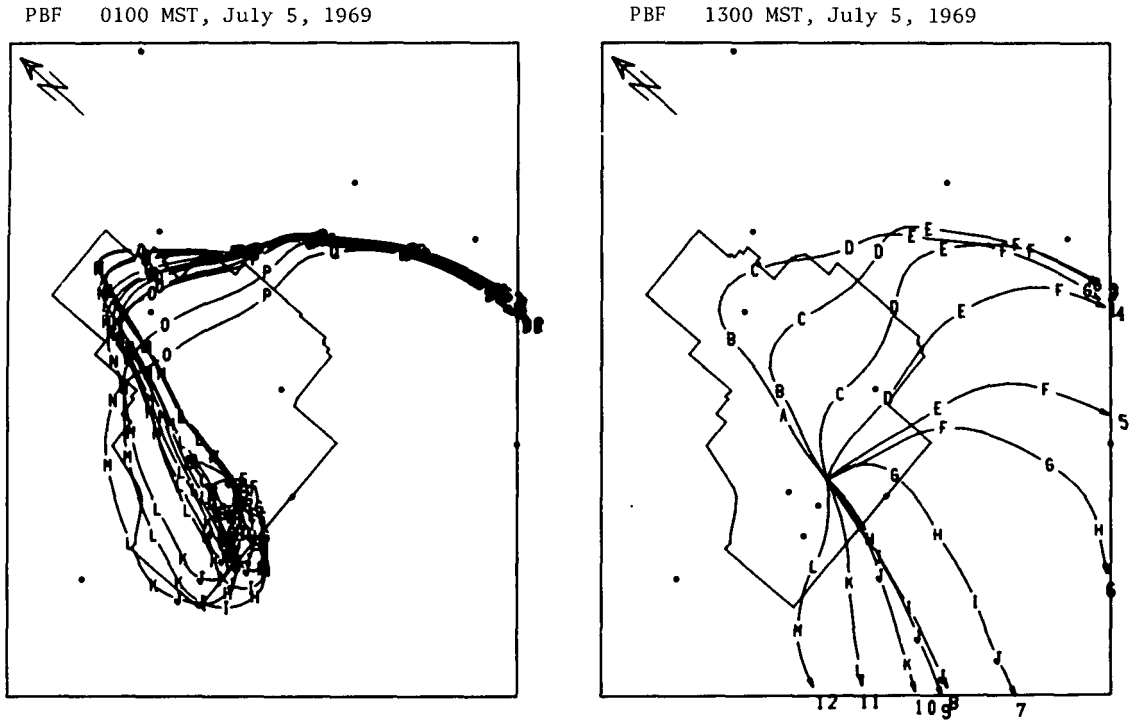

FIGURE 9.—Trajectories of hypothetical particles released hourly and transported by a time series of objectively interpolated wind fields. The numbers at the ends of the trajectories indicate the order of release, and the letters along the trajectories represent hourly positions. (See table 2.)

TABLE 2.—*Symbols for particle trajectories. The particle numbers appear opposite their release times. The hourly particle position is indicated by the appropriate letter-time combination.*

Release duration 0100–1200 MST		Release duration 1300–2400 MST	
1 0100	L 1300	1 1300	L 0100
2 A 0200	M 1400	2 A 1400	M 0200
3 B 0300	N 1500	3 B 1500	N 0300
4 C 0400	O 1600	4 C 1600	O 0400
5 D 0500	P 1700	5 D 1700	P 0500
6 E 0600	Q 1800	6 E 1800	Q 0600
7 F 0700	R 1900	7 F 1900	R 0700
8 G 0800	S 2000	8 G 2000	S 0800
9 H 0900	T 2100	9 H 2100	T 0900
10 I 1000	U 2200	10 I 2200	U 1000
11 J 1100	V 2300	11 J 2300	V 1100
12 K 1200	W 2400	12 K 2400	W 1200

The particles released at the beginning of the period move to the southwest and off the grid, indicating several hours of northeasterly flow from the source to the bottom of the grid. During the release period, however, the direction of motion of the particles suddenly reverses and they stream northeastward until they leave the grid. This trajectory pattern shows a definite preference for the 0100–1200 MST release period when considered over all seasons, probably because of its very strong occurrence during this period for the summer season. It is the most predominant pattern during the summer season for the 0100–1200 MST release period with a 28-percent occurrence. In order of predominance for the 0100–1200 MST releases during the other seasons, it ranks third in the winter, fourth in the spring, and eighth in the fall. The only rankings this pattern has for the 1300–2400 MST release are fourth in the winter and eighth in the spring. This would indicate that the type C pattern is strongly related to the reversal of the winds due to the overall slope of the plain from the northeast to the southwest and the diurnal heating and cooling cycle.

The next pattern, designated type "D," also indicates a change in the flow pattern from northerly or northeasterly flow through southerly flow. The character of this pattern, however, indicates the change to be a gradual clockwise rotation of the wind direction instead of an abrupt reversal as in type C. The trajectory patterns that fall into this type give the first hint of a spatial difference in the winds over the area of concern. The winds near the bottom of the grid seem to be turning before the wind at the source does. The type D pattern also showed a preference for the 0100–1200 MST release time, except for the winter season. Its most frequent occurrence was during the summer season, in which it ranked second behind type C. Its next most frequent occurrence was during the spring, in which it ranked second behind type A. In almost every occurrence of this type, the shift in the wind began between 0900 and 1100 MST.

The next type of trajectory pattern, denoted "E," is characterized by the particles streaming northeastward for the entire release period and leaving the top of the grid. The pattern indicates a sustained flow from a southwesterly direction. The relatively small percentage of the time during which this type occurs through either release period is an indication that, although wind rose information indicates that the wind blows from this sector over 30 percent of the time, it does not do so in a sustained

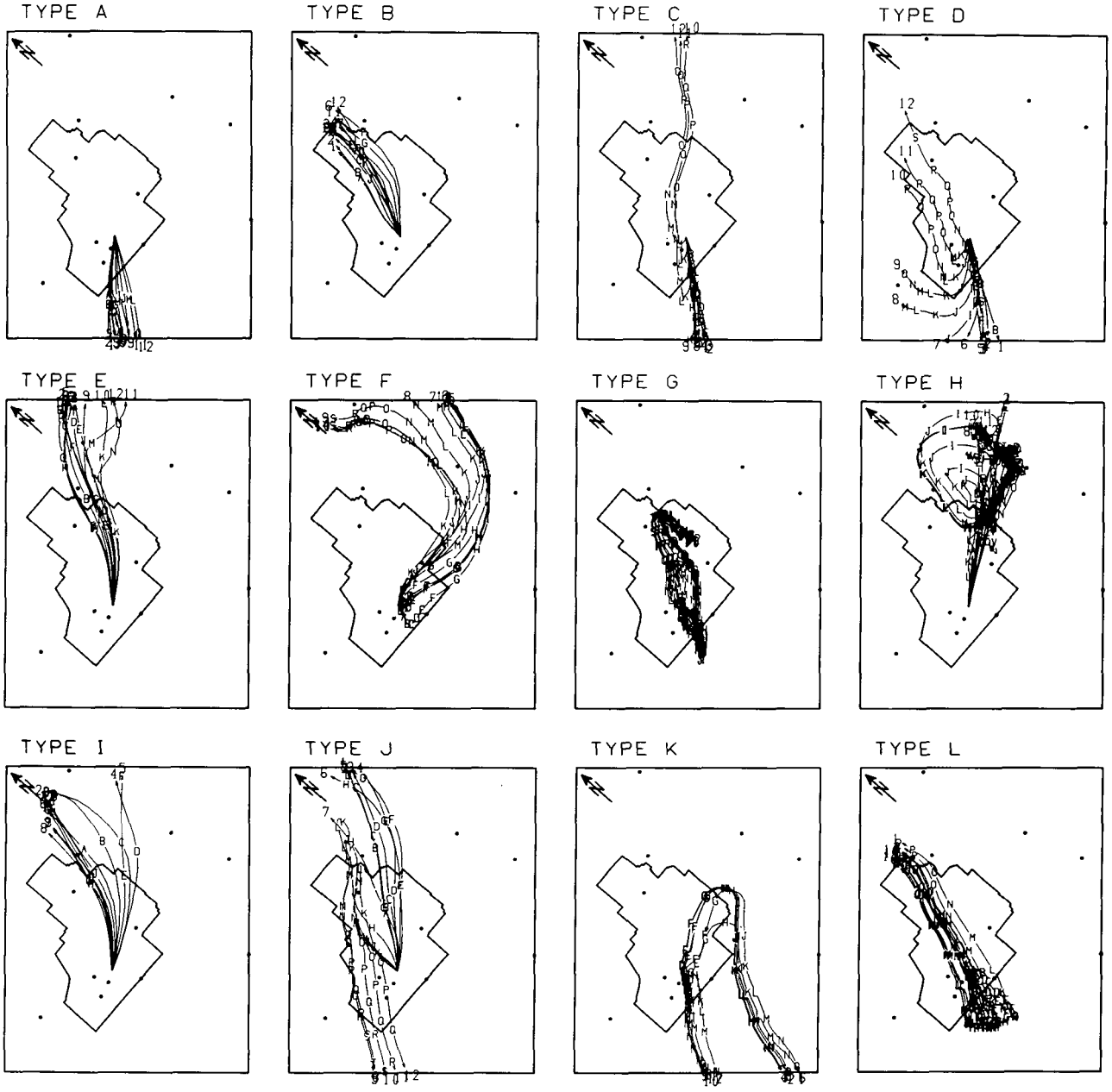

FIGURE 10.—Trajectory patterns typed according to frequency of occurrence. (See table 3.)

manner from the source to the top of the grid. The highest percentage of occurrence for type E is 9 percent for the spring season, in which it ranks third behind types A and D. This seems to contrast with the situation noted for type A, in which there was a very significant amount of sustained northerly flow. There is probably some bias introduced by the fact that the source is twice as far from the top of the grid as it is from the bottom. Also, since type C indicates that the onset of the southerly wind is from 0900 to 1100 MST, a release period from 0900 to 2100 MST would probably show a higher occurrence of type E. One might also suspect that the contrast is due in part to the generally more variable and complex flow characteristics in the upper portion of the grid. This is indicated by some of the types yet to be discussed.

The next pattern shown, denoted type "F," is one that definitely indicates a spatial variation in the flow because the trajectories are curved and show little variation with time. A single curved trajectory may be due either to the rotation of a straight flow pattern with time or to a curved flow pattern that remains stationary with time. This pattern of trajectories indicates flow from a westerly direction at the source becoming southerly toward the top of the grid. The most predominant occurrence of this pattern is in the fall. For the 0100–1200 GMT release period, it occurred during 7 percent of the days and ranked seventh. For the 1300–2400 MST release period, it occurred 8 percent of the days and ranked third. This is the first type to give an indication of the flow conforming to the curved depression in the topography. Releases from a source location in the lower right section of the grid would probably give a much clearer indication.

The next trajectory pattern, denoted "G," is one in which very light winds are indicated. Since none of the

TABLE 3.—*Percentage of occurrence of the trajectory pattern types for the year (numbers in parentheses), for the year according to release (Rlse) period, and seasonally according to release period*

Type		A (20)		B (8)		C (8)		D (7)	
Period	Rlse (MST)	0100	1300	0100	1300	0100	1300	0100	1300
Year		21	18	7	8	12	4	12	2
Winter		30	22	16	16	7	9	3	7
Spring		21	17	3	5	7	5	16	1
Summer		8	7	3	4	28	0	20	1
Autumn		27	26	8	8	6	0	9	0

Type		E (5)		F (4)		G (4)		H (4)	
Period	Rlse (MST)	0100	1300	0100	1300	0100	1300	0100	1300
Year		6	4	4	4	5	3	1	6
Winter		4	4	4	4	6	2	3	7
Spring		9	3	3	5	7	3	0	5
Summer		3	3	3	0	2	1	2	9
Autumn		7	3	7	8	8	6	0	4

Type		I (4)		J (4)		K (3)		L (3)	
Period	Rlse (MST)	0100	1300	0100	1300	0100	1300	0100	1300
Year		4	4	2	5	2	4	5	0
Winter		4	1	6	12	2	4	0	0
Spring		7	8	0	4	3	8	0	0
Summer		5	4	3	13	1	2	11	2
Autumn		0	1	1	0	0	1	9	2

12 particles released is carried off the grid, the winds were light and variable for at least 24 hr. The summer season shows the least percentage of occurrence of this pattern. This is probably a result of the predominance of the diurnal up-valley–down-valley flow. The other three seasons show 6- to 7-percent occurrences of type G for the 0100–1200 MST releases and 2- to 6-percent occurrences for the 1300–2400 MST releases. This indicates that a light and variable wind situation in the central portion of the grid has a stronger tendency to persist for 24 hr if it begins at 0100 MST than if it begins at 1300.

The trajectory pattern, denoted type "H," is one of the most striking examples of spatial variation in the wind flow. This type is a manifestation of the circular eddy that was discussed in the previous section. The occurrence of this type shows a definite bias toward the 1300–2400 MST release period, indicating that it is a late evening or early morning phenomenon. It occurs most frequently (9 percent) in the summer and ranks second behind type C, but the next highest occurrence (7 percent) of the phenomenon is in winter and ranks fifth. This trajectory pattern is probably the most dramatic in demonstrating the contrast between the type of transport that might be deduced from a wind observation at the source and several observations over the entire area of interest.

The next three patterns shown, denoted "I," "J," and "K," show why type E does not occur more often than a wind rose would imply. Type I indicates southwesterly flow from the source becoming southerly about 90 km northeast of the source. The percentages shown indicate this condition to be most predominant in the spring. Type J indicates southwesterly flow throughout the release period followed by a sudden reversal to northeasterly flow. The percentages shown indicate that it is most predominant during the 1300–2400 MST release and that it occurs most often during the summer and winter seasons. The relatively high percentage (13 percent) in the summer would be more than likely due to the diurnal wind reversals while the correspondingly high occurrence in winter probably would be due to frontal passages. Type K also indicates a southeasterly flow reversing to a northeasterly direction. The difference is that the direction change occurs earlier during the release period and it occurs as a gradual clockwise rotation. This type also shows a preference for the 1300–2400 MST release, but it occurs most frequently (8 percent) during the spring season in contrast to the summer and winter highs of type J.

The last type shown is designated "L" and also indicates a reversal in the flow pattern. The trajectory pattern in this case indicates a light northerly flow changing to a stronger southerly flow in such a way that the particles are swept back across the grid in a line. This pattern shows a definite bias toward the 0100–1200 MST release period. It occurred only during the summer (11 percent), in which it ranked third behind types C and D, and during the fall (9 percent), in which it ranked third behind types A and D.

Other types of patterns are recognizable, but they occur with less frequency than those shown. On an annual basis, the 12 types shown account for about 74 percent of the flow patterns observed. The variability in the trajectory patterns seems to be greatest for the 1300–2400 MST release period during the spring, summer, and fall seasons. It would be during this release period that the approximation of the wind field by the source wind would be the least desirable.

As an example of what can happen when the source wind is used to approximate the wind over an area of the size we are dealing with here, trajectories have been computed over selected release periods using the wind from all the stations and, from the wind at the source, applied over the whole grid. The resulting trajectory patterns are shown in figure 11. The trajectories in the upper diagrams (fig. 11A) were obtained using the wind field data. The trajectories in the lower diagrams (fig. 11B) were obtained for the corresponding release times using the source wind only. The contrast resulting from the two methods is quite evident for these cases.

7. CONCLUDING REMARKS

One of the major objectives of this investigation is to evaluate the technique of using objective analyses of wind data from a network of towers to examine the spatial and temporal variation in mesoscale flow patterns over a particular area. The technique of streamline analysis of wind observations from a large-scale network has long been

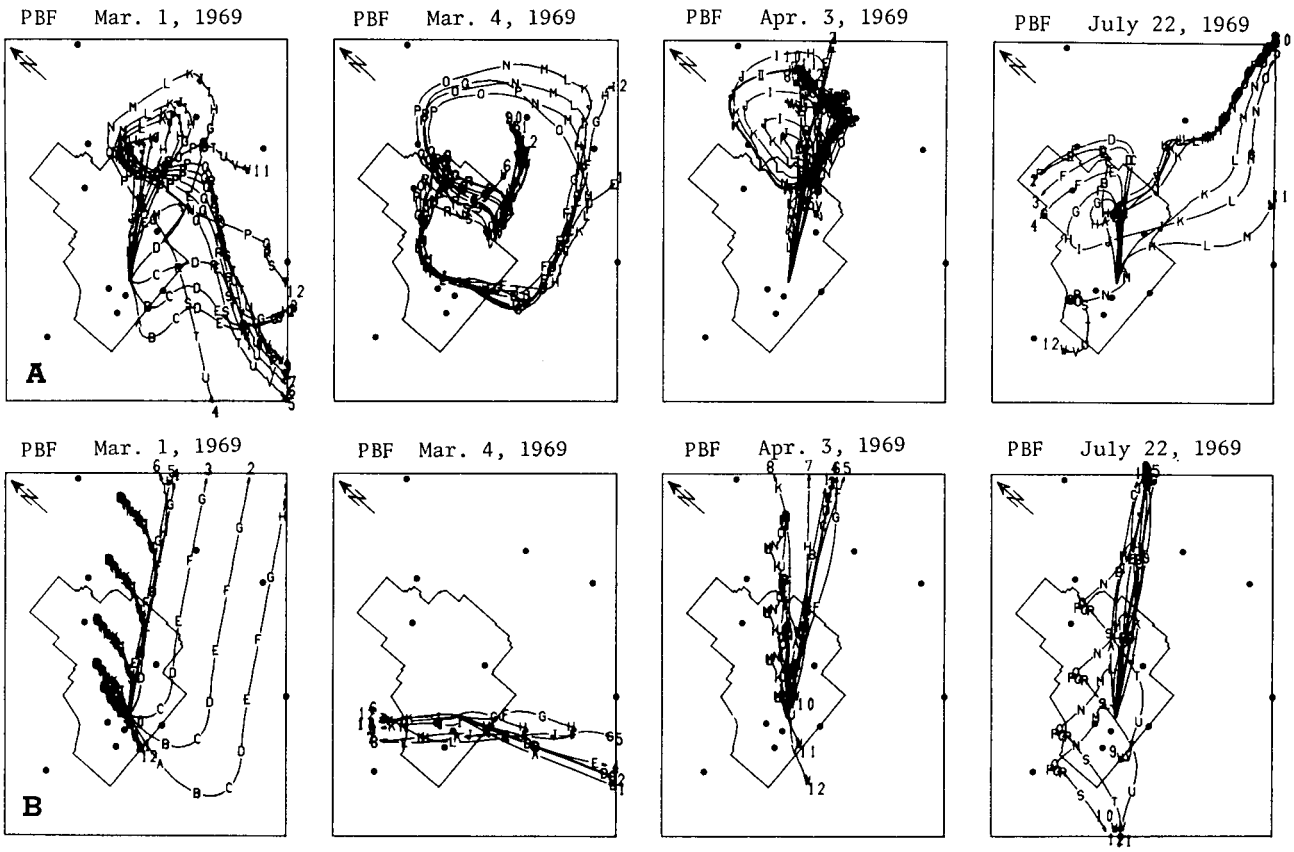

FIGURE 11.—Comparison of (A) trajectories derived from the wind field with (B) trajectories derived from the source wind applied over the whole grid for the corresponding time periods (1300 MST on days indicated).

useful, especially in the Tropics. The problem to be considered is whether or not there is, in general, enough spatial variation in the wind over an area of intermediate size to warrant observations from more than one location. A very cursory examination of the wind field plots for 1969 indicates that the data from a single station are representative over the whole area for only a small percentage of the time. Not only is the uniformity of the flow disturbed randomly by frontal systems or thunderstorms moving through the area, but it is regularly disturbed by flow that appears to be strongly correlated with a minor but very distinctive topographic variation over the expanse of the area of concern. The combination of the topographic variation and the diurnal heating cycle seems to be a major factor in the formation of a circular eddy that occasionally forms and persists for a few hours in the upper portion of the plain.

The dynamic causes for these phenomena can only be inferred at this point, but their existence has been confirmed through the examination of the wind field plots. Their existence could not be determined from wind rose or time-series analyses of the data from a single section. Wind rose analyses of the data from all the stations are also inadequate in distinguishing flow patterns. Time-series analysis of the data from the network, however, might provide valuable quantitative information about the spatial and temporal variation in the flow. Regardless of the outcome of this type of analysis or any other type of quantitative analysis of the network winds, the technique of systematically displaying the data, along with an objective analysis for subjective examination, shows promise of being a valuable tool for a preliminary analysis of wind data from any area. The microfilm recording of cathode-ray tube plots makes the process economically feasible.

Another major objective of this investigation is to examine the implications of the wind fields on the transport of material in the layer in which these measurements are representative. The fact that the wind field observations indicate significant spatial variation in the flow during some period of over half the days of the year would strongly suggest that estimates of the transport of materials with winds from a network of observations would be somewhat better than estimates based on an observation from a single location. The few selected cases, in which the trajectory patterns constructed with both types of data are compared, show how great the discrepancy can be.

The construction of the trajectories of particles released from the same location once an hour, and displaying them 12 at a time for a long period, provides information concerning the time changes and some of the spatial variation in the flow patterns in a more compact form than the wind field plots. The subjective typing of these trajectory patterns provides unique information about the possible influence of the area flow patterns on transport from a selected source location. The sample examined here is not large enough to be considered a climatology, but the results obtained do provide an indication of the types of

transport patterns that might be expected during each of the four seasons. For example, the winter season exhibits sustained homogeneous flow from the release point to the bottom and left side of the grid for about 40 percent of the days (types A and B), but the other seasons indicate more temporal and spatial variation in the flow. Trajectory plots of the kind used in this analysis depict the nature of this variation to the extent that one can distinguish between two types of wind reversals as in types C and D. The distinction can be very important when one is concerned with the transport of an effluent.

This brings us to the question of how well these trajectories represent real atmospheric transport. One would certainly suspect that, under conditions of strong instability in which material would be carried well above the height of the towers, large discrepancies could easily occur. However, during stable conditions, much of the material released will remain in the layer represented by the tower measurements. There is evidence of this during episodes of brush and field fires in the autumn. Also, during the winter, a plume of NO_2 from a stack in the south-central portion of the test site is often observed to be trapped under a low inversion and extends beyond the large butte marked C in figure 2. Under these conditions, the tower winds should give a reasonable estimate of the transport and, generally, a much better estimate than one from a single station.

ACKNOWLEDGMENTS

Grateful acknowledgment is expressed to the members of the Air Resources Laboratories, Field Research Office staff, for their invaluable assistance and cooperation in this work. The establishment of the offsite network of wind stations was accomplished by C. R. Dickson, F. E. White, and G. E. Start. Lydia Thorngren typed the manuscript.

REFERENCES

Angell, James K., Pack, Donald H., and Dickson, C. Ray, "Lagrangian Study of Helical Circulations in the Planetary Boundary Layer," *Journal of the Atmospheric Sciences*, Vol. 25, No. 5, Sept. **1968**, pp. 707–717.

Blackadar, Alfred K., "Boundary Layer Wind Maxima and Their Significance for the Growth of Nocturnal Inversions," *Bulletin of the American Meteorological Society*, Vol. 38, No. 5, May **1957**, pp. 283–290.

Bonner, William D., and Paegle, Jan, "Diurnal Variations in the Boundary Layer Winds Over the South-Central United States in Summer," *Monthly Weather Review*, Vol. 98, No. 10, Oct. **1970**, pp. 735–744.

Brown, R. A., "A Secondary Flow Model for the Planetary Boundary Layer," *Journal of the Atmospheric Sciences*, Vol. 27, No. 5, Aug. **1970**, pp. 742–757.

Ching, Jason K. S., and Businger, Joost A., "The Response of the Planetary Boundary Layer to Time Varying Pressure Gradient Force," *Journal of the Atmospheric Sciences*, Vol. 25, No. 6, Nov. **1968**, pp. 1021–1025.

Endlich, Roy M., and Mancuso, Robert L., "Objective Analysis of Environmental Conditions Associated With Severe Thunderstorms and Tornadoes," *Monthly Weather Review*, Vol. 96, No. 6, June **1968**, pp. 342–350.

Gee, J. H., "A Note on the Effect of Directional Wind Shean or Medium-Scale Atmosphere Diffusion," *Quarterly Journal of the Royal Meteorological Society*, Vol. 93, No. 396, London, England, Apr. **1967**, pp. 237–241.

Hanna, Steven R., "The Formation of Longitudinal Sand Dunes by Large Helical Eddies in the Atmosphere," *Journal of Applied Meteorology*, Vol. 8, No. 6, Dec. **1969**, pp. 874–883.

Hilsmeier, William F., and Gifford, Frank A., "Graphs for Estimating Atmospheric Dispersion," U.S. Atomic Energy Commission *Report* ORO–545, Weather Bureau, Oak Ridge, Tenn., **1962**, 10 pp.

Hoecker, Walter H., Jr., "Three Southerly Low-Level Jet Systems Delineated by the Weather Bureau Special Pibal Network of 1961," *Monthly Weather Review*, Vol. 91, Nos. 10–12, Oct.–Dec. **1963**, pp. 573–582.

Hoecker, Walter H., "Comparative Physical Behavior of Southerly Boundary-Layer Wind Jets," *Monthly Weather Review*, Vol. 93, No. 3, Mar. **1965**, pp. 133–144.

Mancuso, Robert L., and Endlich, Roy M., "Sequence of Meteorological Analyses for Southeast Asia Produced by Computer," *Final Report*, Contract No. DAAB07–69–C–0415, Stanford Research Institute, Menlo Park, Calif., July **1970**, pp. 1–11.

Pasquill, Frank, "Some Observed Properties of Medium Scale Diffusion in the Atmosphere," *Quarterly Journal of the Royal Meteorological Society*, Vol. 88, No. 375, London, England, Jan. **1962**, pp. 70–79.

Saffman, P. G., "The Effect of Wind Shear on Horizontal Spread From an Instantaneous Ground Source," *Quarterly Journal of the Royal Meteorological Society*, Vol. 88, No. 378, London, England, Oct. **1962**, pp. 382–393.

Shephard, Donald, "A Two-Dimensional Interpolation Function for Irregularly Spaced Data," *Proceedings of the 23d Association for Computing Machinery National Conference, Las Vegas, Nevada, Aug. 27–29, 1968*, Brandon/System Press, Inc., Princeton, N.J., Aug. **1968**, pp. 517–524.

Slade, David H. (Editor), *Meteorology and Atomic Energy, 1968*, 2d Edition, U.S. Atomic Energy Commission, Division of Technical Information, Oak Ridge, Tenn., July **1968**, 445 pp.

Smith, F. B., "The Role of Wind Shear in Horizontal Diffusion of Ambient Particles," *Quarterly Journal of the Royal Meteorological Society*, Vol. 91, No. 389, London, England, July **1965**, pp. 318–329.

Van der Hoven, Isaac (Editor), "Atmospheric Transport and Diffusion in the Planetary Boundary Layer," *ESSA Technical Memorandum*, ERLTM–ARL 9, U.S. Department of Commerce, Air Resources Laboratories, Silver Spring, Md., Dec. **1968**, 60 pp.

Van der Hoven, Isaac (Editor), "Atmospheric Transport and Diffusion in the Planetary Boundary Layer," *ESSA Technical Memorandum*, ERLTM–ARL 14, U.S. Department of Commerce, Air Resources Laboratories, Silver Spring, Md., June **1969**, 44 pp.

Wendell, Larry L., "A Preliminary Examination of Mesoscale Wind Fields and Transport Determined from a Network of Wind Towers," *NOAA Technical Memorandum*, ERLTM–ARL 25, U.S. Department of Commerce, Air Resources Laboratories, Silver Spring, Md., Nov. **1970**, 27 pp. plus appendixes.

[*Received June 21, 1971; revised March 9, 1972*]